Dissipation of the excitation front as a mechanism of self-terminating arrhythmias

I.V.Biktasheva*, V.N.Biktashev[1,2], W.N.Dawes,
A.V.Holden[3], R.C.Saumarez, A.M.Savill

December 6, 2002

CFD Laboratory, Department of Engineering, University of Cambridge, Trumpington Street, Cambridge CB2 1PZ, UK

[1] Department of Mathematical Sciences, Liverpool University, Mathematics & Oceanography Building, Peach Street, Liverpool, L69 7ZL, UK

[2] On leave from: Institute for Mathematical Problems in Biology, Russian Academy of Sciences, 142292 Pushchino, Moscow region, Russia

[3] School of Biomedical Sciences, Worsley Building, Leeds University, Leeds LS2 9JT, UK

* Corresponding author. Current address: Department of Computer Science, University of Liverpool, Chadwick Building, Peach Street, Liverpool L69 7ZF, UK

Abstract

The *dissipation of the excitation wavefronts* is a specific mechanism of propagation failure if the sharp gradient of the transmembrane voltage at the wavefront smears out and spread of voltage becomes diffusive, as the main excitation current becomes inactivated. This is produced by the normal kinetics of the ionic currents underlying the action potential. Here we demonstrate that the dissipation of the excitation wavefront can cause arrhythmia as well as lead to its self-termination. We use Courtemanche et al. model of human atrial action potential to demonstrate how re-entry creates dynamic electrophysiologic inhomogeneity of the tissue. Local dissipation of the excitation front cause wave breaks and instantaneous displacement of the tip of the re-entry, and the same mechanism can lead to elimination of all wavelets, as the inhomogeneity creates conditions for simultaneous dissipation of their excitation fronts.

Key words: human atrium, self-terminating arrhythmias (mechanism), fast sodium current, spiral wave, computer modelling.

1 Introduction.

Most modern theories of ventricular and atrial fibrillation (Panfilov & Pertsov 2001, Jalife, Berenfeld & Mansour 2002) consider them as conditions that persist unless terminated by external intervention, see e.g. the title of (Weiss, Chen, Qu, Karagueuzian & A. 2000): "Ventricular fibrillation: How do we stop the waves from breaking?". However, continuous monitoring of coronary-care unit patients reveals episodes of self-terminating atrial and ventricular arrhythmias (Clayton, Murray, Higham & Campbell 1993, Cobbe 1997, Makikallio, Huikuri, Myerburg, Seppanen, Kloosterman, Interian, Castellanos & Mitrani 2002).

An important feature of an excitation wave in cardiac tissue is that it will fail to propagate if the spatial and temporal gradients of voltage at the front is too small to excite the tissue ahead of it, and a mathematical theory for this phenomenon has been proposed (Biktashev 2002, Biktashev 2003). The theory predicts that the spectrum of possible propagation speeds is bounded from below, causing a front to dissipate if it is not allowed to propagate quickly enough. A crucial role

is played by the fast Na current inactivation gates h, even if their dynamics are by an order of magnitude slower than those of the voltage.

Dissipation of the excitation wavefronts can be a decisive factor not only in initiation of a re-entry, but also its self-termination. We use a model of human atrial action potential (Courtemanche, Ramirez & Nattel 1998) (hereafter referred to as CRN model) to demonstrate how a re-entry spontaneously creates and enhances dynamic electrophysiologic inhomogeneity of the tissue, which eventually leads to simultaneous dissipation of the excitation fronts of all existing wavelets.

We have performed 7 numerical experiments with the model, with different initial conditions. In all of them, the re-entry self-terminated. The difference in initial conditions led to different dynamic electrophysiologic inhomogeneities of the medium and, consequently, the time of self-terminating of the spirals ranged between 1.018s and 8.83s. We present in detail the two extreme examples, and a brief description of the others.

2 Materials and methods: 2D model of human atrial tissue.

We used the human atrial action potential model by Courtemanche et al. (1998) (CRN model) incorporated into a two-dimensional reaction-diffusion system of partial differential equations, in the same way as e.g. (Biktashev & Holden 1996). The diffusion coefficient of the transmembrane voltage $D = 0.03125\,\mathrm{mm^2 s^{-1}}$ was set to give a plane wave velocity of $\approx 265\,\mathrm{mm/s}$. The partial differential equations were solved with time step $\Delta t = 0.1$ms, space step $\Delta x = 0.2$mm and non-flux boundary conditions. The medium was isotropic and of 75×75 mm. This focuses on the excitation and propagation kinetics and ignores the additional complications due to geometry, anisotropy and heterogeneity of a real atrium.

Spiral waves were initiated by the phase distribution method, as described in (Biktashev & Holden 1998*b*). This method produces a spiral wave at a prescribed location and avoid introducing into the initial conditions inhomogeneity typical for other methods such as cross-field stimulation or temporary propagation block. The pitch (radial distance between successive wavefronts) of the Archimedean spiral in all cases was 80 mm.

The tip of the spiral wave was defined as an intersection of isolines $V = -40$ and $o_i = 0.5$, where o_i is the inactivation gate of the I_{to} current. The moment of self-termination of the arrhythmia was defined as the moment of ultimate disappearance of all tips.

The pseudo-ECG signals were calculated as weighted averages of the transmembrane voltage (Gulrajani 1998),

$$E_j(t) = \int w_j(x,y) V(x,y,t)\,\mathrm{d}x\mathrm{d}y$$

where instead of the weights $w_j(x,y)$, depending on the geometry of the heart, electric properties of surrounding tissues and position of recording electrodes, we choose the weights in very simple forms,

$$w_1(x,y) = 1, \qquad w_2(x,y) = \begin{cases} 1, & x > x_*, \\ -1, & x < x_*, \end{cases} \qquad w_3(x,y) = \begin{cases} 1, & y > y_*, \\ -1, & y < y_*, \end{cases}$$

where $x_* = (x_{\min} + x_{\max})/2$, $y_* = (y_{\min} + y_{\max})/2$ are the coordinates of the centre of the medium. This choice of simple weighting functions corresponds to the simplified idealisation of the simulations, which neglect the realistic geometry, heterogeneity and anisotropy of the atrium. We calculate and present three different pseudo-ECG signals (which may be thought of as corresponding to the different ECG leads), to ensure that the qualitative information on the excitation field evolution is represented faithfully and is not an artefact of the choice of a particular weighting function.

3 Results.

We demonstrate here the results of two selected numerical experiments, which differ only by their initial spiral wave solutions, and due to only this difference in initial conditions different dynamic

electrophysiologic al inhomogeneities of the medium develop leading to different scenario of the spirals self-termination. The main points are:

- The spiral wave itself creates dynamic electrophysiological inhomogeneity of the medium.
- The inhomogeneity is a result of a number of inter-related processes including triggered recovery of some parts of the medium, "germination" of the tip of the spiral into early recovered parts of the tissue, and dissipation of the excitation front.
- These processes result from the kinetics of the ionic currents underlying the action potential, and eventually lead to self-termination of the re-entry.

Experiment A. To initiate a spiral, the phase distribution method uses one-dimensional calculations to record values of all dynamical variables in a plane periodic wave as functions of single scalar variable, the phase. To create the spiral, a distribution of the phase over the plane, corresponding to an Archimedean spiral with an appropriate wavelength, is used to specify the distribution of the dynamic variables via these functions. In this experiment the phase data were produced by 5 pulses with the period of 1000 ms.

Triggered recovery effect. This term was used in (Leon, Roberge & Vinet 1994, Nygren, Leon & Giles 2001) to describe recovery of sites within the excitation wave before the "tail" of the excitation wave arrives at that site. This creates recovered gaps amid still excited tissue and fragments excited regions. We observed two such events during the experiment. Both of them were due to the rate dependence of the action potential duration. The first one starts to appear after $\approx$ 160 ms, is clearly seen at 200 ms, and completely finishes by $\approx$ 300 ms (see fig. 1). It was due to combination of the width of the initial spiral, and the fact that the action potential duration is bounded and for the CRN model cannot be more than $APD_{50\_max} \approx 180$ ms. The area affected by the triggered recovery during this episode is comparable to the size of the whole tissue and creates a large spatial electrophysiological inhomogeneity, which is important for the following events.

The second event of the triggered recovery starts after $\approx$ 440 ms. One can see that the first triggered recovery area repeats the original shape of the spiral, compare 200ms and 400ms frames in fig. 1, and the second triggered recovery area repeats the form of the spiral at 360ms, see 360ms and 560ms frames in fig. 1. Notice that in both cases the triggered recovery does not directly lead to the spiral wave breaks, contrary to what was suggested in (Nygren et al. 2001, Leon et al. 1994). Instead, the process effectively leads to dynamic adjustment of the wavelength and creates dynamic electrophysiological inhomogeneity of the medium.

"Germination" of the spiral wave tip into the early recovered parts of tissue, i.e. lengthening of the front due to sideward movement of the tip.

This effect can be seen in many frames in fig. 1. It follows early recovery of the medium in the vicinity of the tip of the re-entry due to either previous block of the area for excitation or the triggered recovery effect, and results in the parts of the trajectory of the tip with the biggest curvature. The sideward advancement of the spiral wave tip, tangentially to the direction of the front propagation, leads to wavefronts propagating with different speeds through different pathways compared to the previous turn of the re-entry, changing the refractory pattern and thus contributes to the enhancement of the dynamic inhomogeneity.

The trajectory of the spiral wave tip for the first 620 ms of the experiment is shown in fig. 6(a). It is confined to the central part of the medium of $\approx$ 25 mm in diameter. The extent of the tip meander and its shape result from the dynamic inhomogeneity of the medium, and, in turn, contribute to the enhancement of this inhomogeneity.

Local dissipation of the wave front. The first local dissipation of the wave front in the vicinity of the core of the spiral starts after 224 ms of the experiment (see fig. 1) and is due to the propagation block by the tail of the spiral. The local front dissipation leads to the break of the spiral and birth of the short piece of the front moving towards the spiral centre, which later dissipates as well. The new tip of the spiral emerges at the other end of the dissipating interval of the excitation

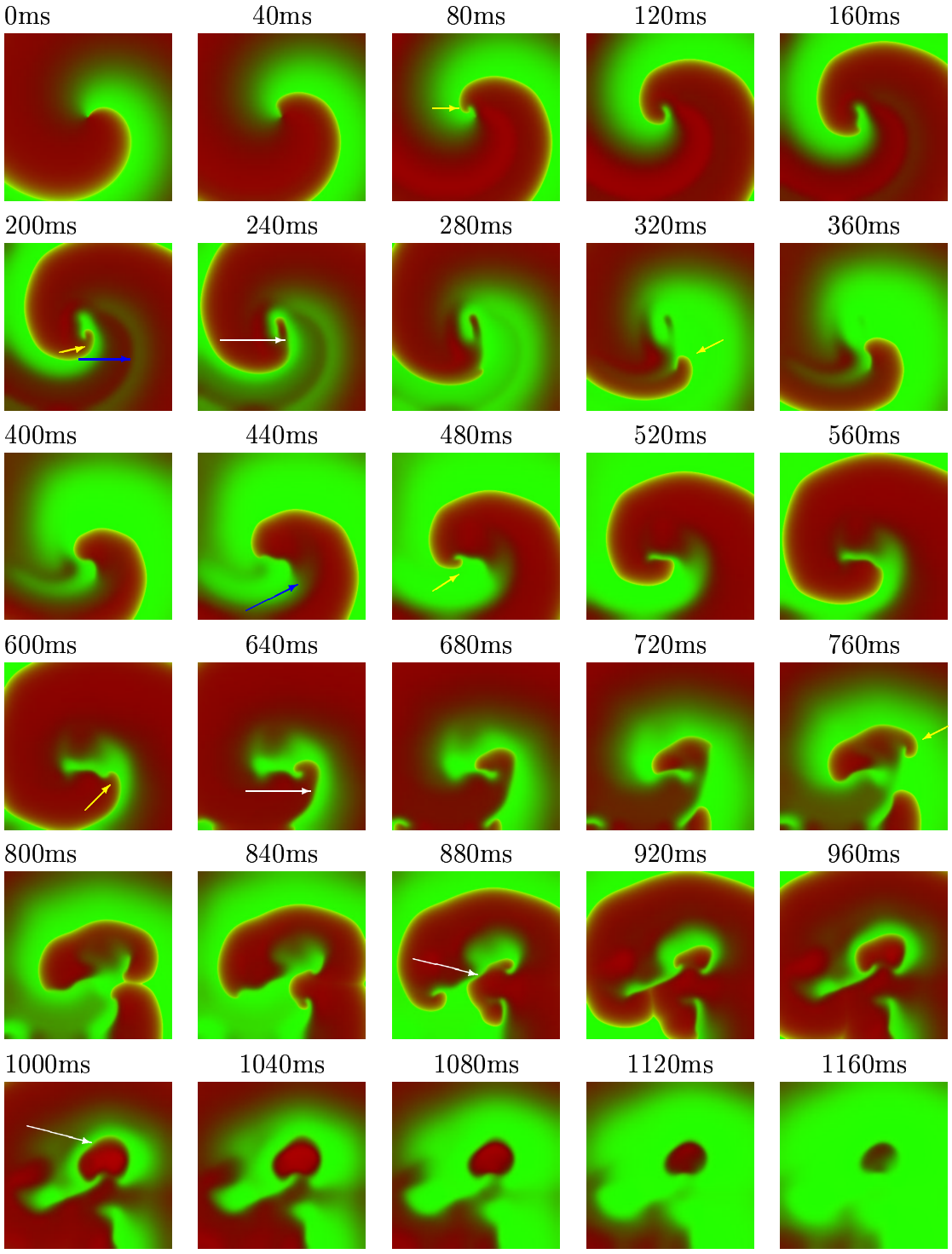

Figure 1: Self-terminating arrhythmia in the 2D human atrium model. Experiment **A**. The blue arrows indicate beginnings of the "triggered recovery". The short yellow arrows indicate beginnings of the sideward movement of the spiral wave tips into the early recovered parts of the medium. The long white arrows indicate beginnings of the excitation front dissipation.

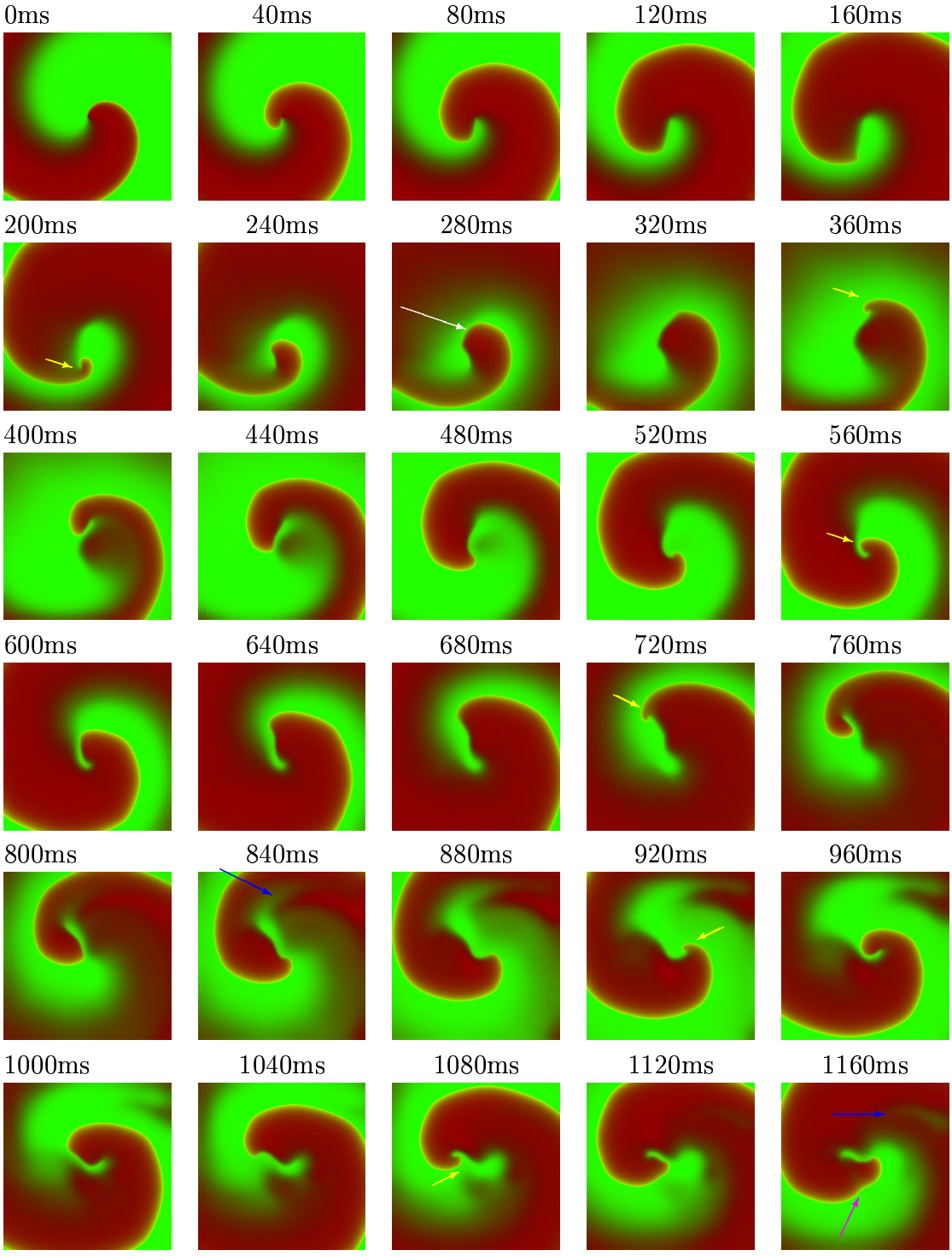

Figure 2: Beginning of the experiment **B**. The blue arrows indicate beginnings of the "triggered recovery". The short yellow arrows indicate beginnings of the sideward movement of the spiral wave tips into the early recovered parts of the medium. The long white arrows indicate beginnings of the excitation front dissipation. The magenta arrow indicates the excitation front concavity due to previous slow down of propagation in this direction.

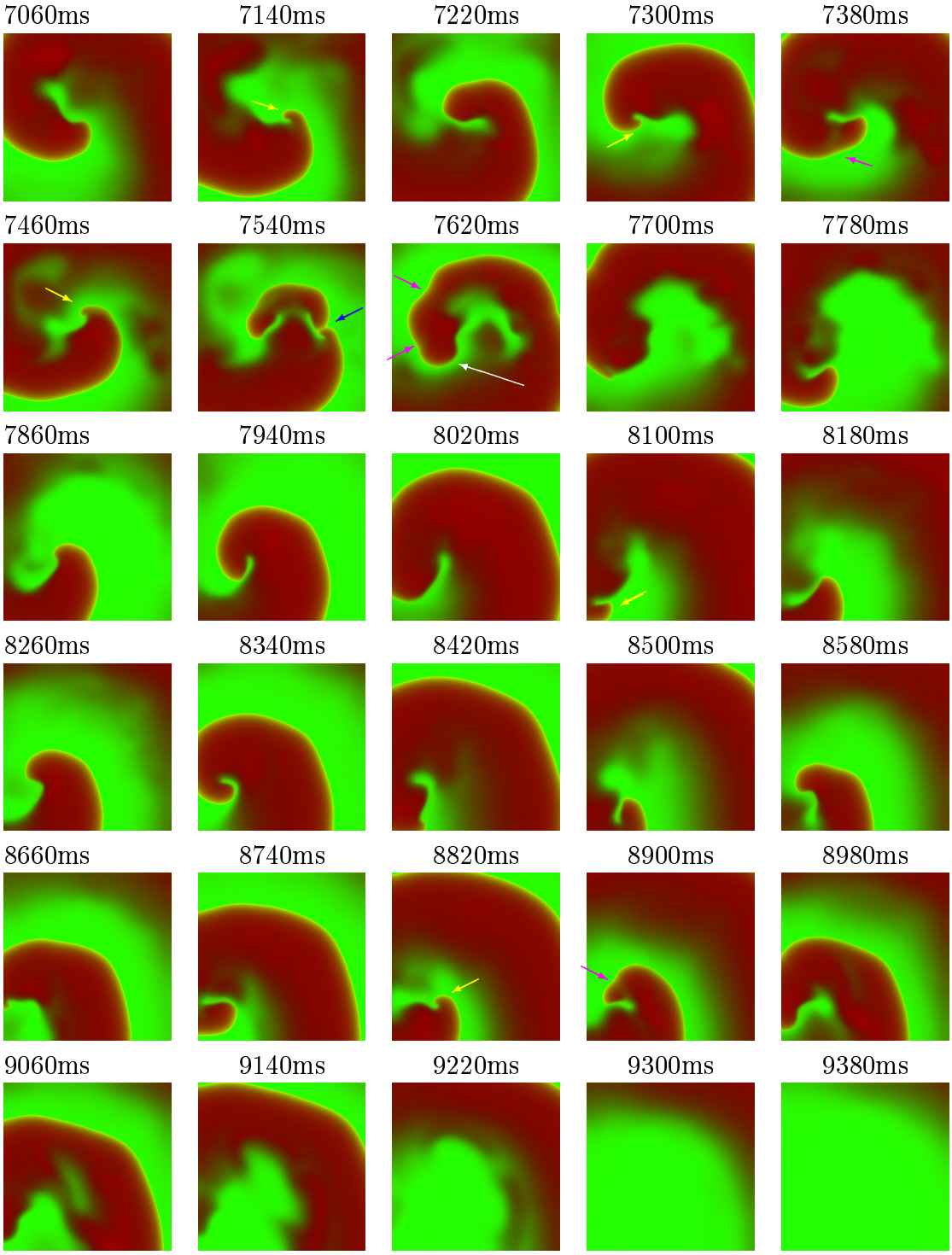

Figure 3: End of the experiment **B**. Random triggered recovery episodes create dynamic electrophysiological inhomogeneity of the medium. The yellow arrows indicate beginnings of the spiral wave tip "germination" into early recovered parts of the medium. The white arrow indicates one of the beginnings of the excitation front dissipation. The magenta arrows indicate the concavities of the excitation front due to previous slow down of propagation in particular directions. The blue arrow indicates the break of the excitation front due to its local dissipation.

front, where propagation is still possible (see 280 ms panel in fig. 1). This effectively means an *instantaneous displacement of the spiral wave tip* from the area with the block of propagation to the recovered piece of tissue, which is able to propagate the excitation front at the moment.

The second case of local dissipation of excitation front starts at about 624 ms. This time, the break of the spiral gives birth to the short piece of the front with two tips in the center of the tissue, which is already repolarised area by the time, and a new tip of the spiral develops from the tissue border (see 680 ms panel in fig. 1). So on the 760 ms panel there are already three leading tips. Later the new waves of excitation interact with each other, developing into a complex quasi-fibrillating pattern. Combination of the birth of new spiral wave tips due to the local dissipations of the excitation front and their "germination" into all possible propagation areas eventually results in the situation, when there is no more recovered tissue to propagate into, which leads to global dissipation of all pieces of the excitation front and subsequent repolarisation of the whole medium.

It has taken a little more than 1s in total from the beginning of the experiment as the onset of the re-entry through the development of quasi-fibrillation to complete repolarisation of the whole medium.

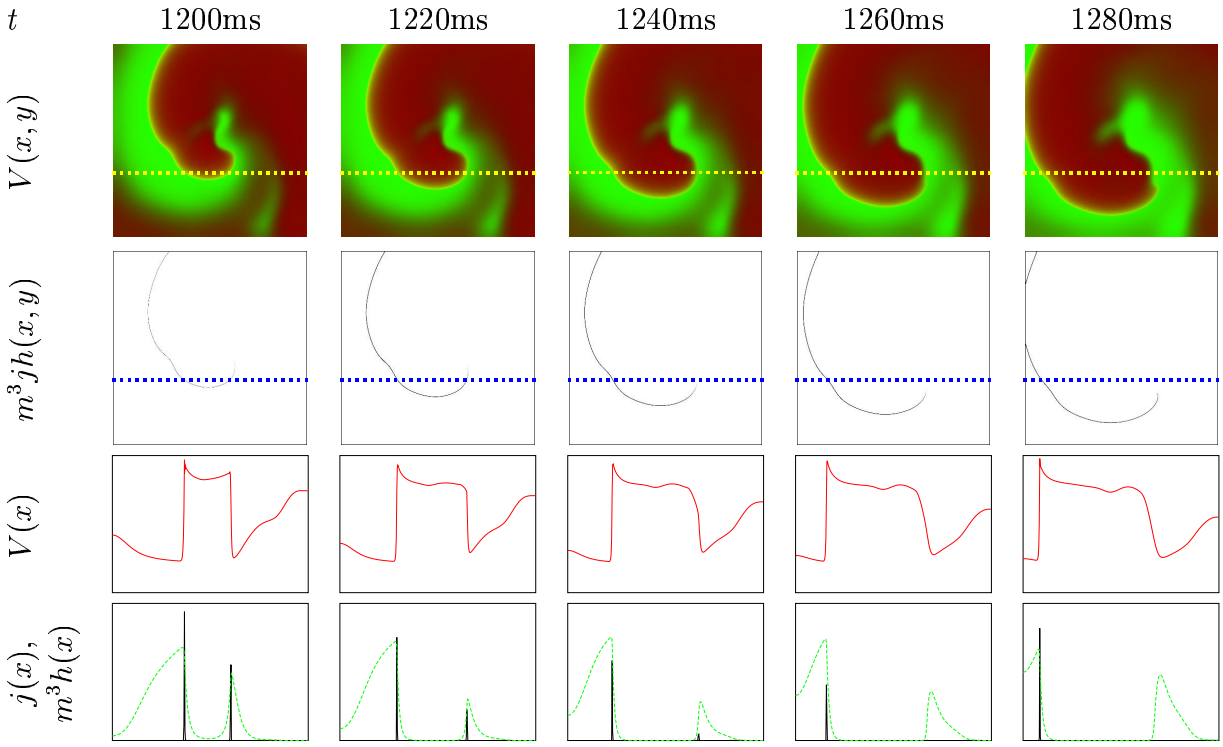

Figure 4: Dissipation of the excitation wavefront causing its shortening with the instantaneous displacement of the tip. Details of an episode from the experiment **B**. Upper row: density plots of the distribution of the transmembrane voltage. Second row: density plots of the distribution of the permeability of the fast Na channels. Third row: profiles of the transmembrane voltage along the dashed line on the density plot. Fourth row: profiles of the m^3h (black solid lines) and j (dotted green lines) factors of the Na channels permeability. The rightward wave has dissipated shortly after 1240 ms, while the leftward wave has successfully overcome a temporary difficulty, showing as a decrease of the Na current at 1260 ms, caused by the previous local slow down of the front resulted in the front temporal local concavity seen in the 1200 ms frame.

Experiment B Here the phase data were initiated by pacing with interval 300 ms during 30 s.

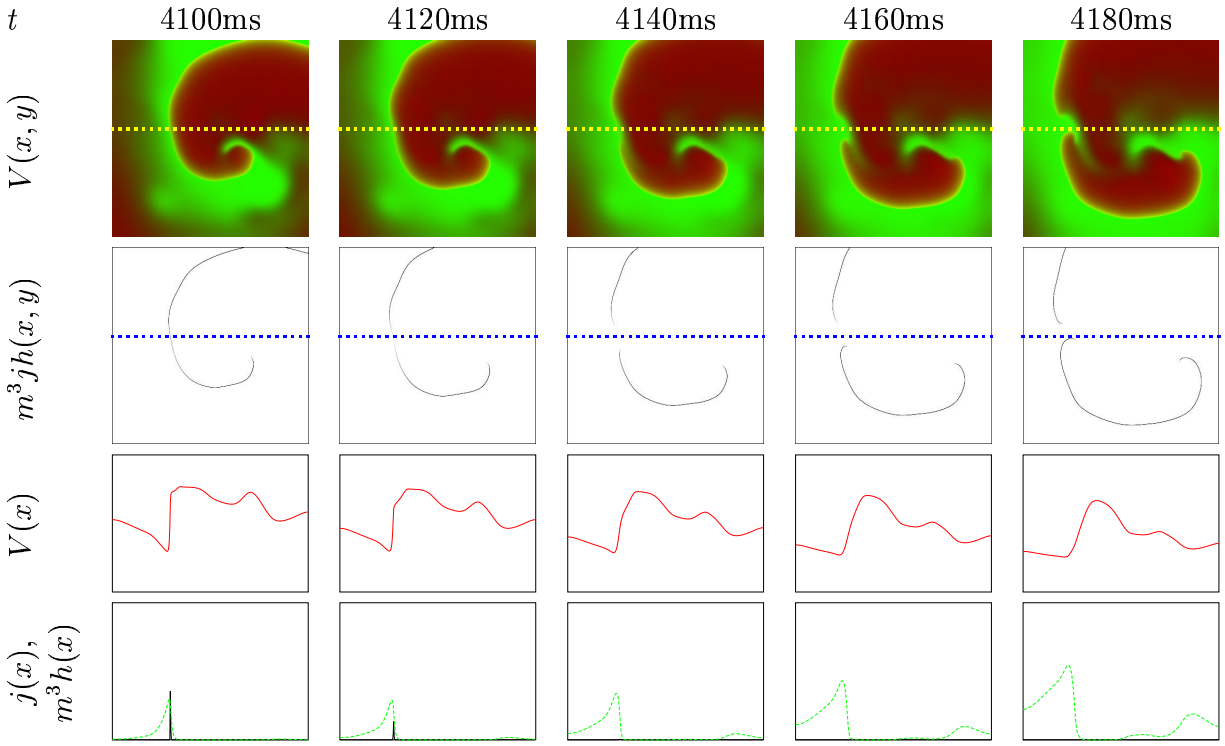

Figure 5: Dissipation of the excitation wavefront, during the experiment **B**, causing its breakup. Notations are the same as on fig. 4. The m^3h profiles show that the front propagating leftward has dissipated at the cross-section line shortly after 4120 ms.

Triggered recovery effect. Triggered recovery starts to appear after 800 ms since the beginning of the experiment (see fig. 2), and results from the complex trajectory of the spiral wave tip, as different parts of the tissue undergo different time patterns of excitation. The area affected by triggered recovery during this first episode is small and located nearby the border of the tissue, so the electrophysiological inhomogeneity, which it creates, does not immediately affect the evolution of the spiral. However, it is the first of a series of triggered recovery episodes occurring at irregular times that creates the dynamic electrophysiological inhomogeneity of the whole medium seen by 7460 ms of the experiment in fig. 3.

The triggered recovery episode close to the spiral wave tip in the frame 7380 ms, fig. 3 occurs across almost the whole wavelength of the spiral, but does not lead to the break of the spiral, see the next 7460 ms frame in fig. 3.

"Germination" of the spiral wave tip into the early recovered parts of tissue. The sideward movements of the spiral wave tips into recovered parts of the medium are seen in many frames in figs. 2 and 3. Initially, the phenomenon does not play any essential role, but near the end of the experiment, it helps the spiral to survive several times, when it almost has died on the border of the medium, see frames 8100 ms, 8420 ms, and 8660 ms in fig. 3.

Local dissipation of the wave front. The wave front local dissipation in the vicinity of the spiral wave tip due to block of propagation results in many instantaneous displacements of the tip during the experiment. The corresponding linear intervals in the trajectory of the spiral wave tip are well seen in fig. 6(b). The breaks of the spiral due to local dissipation of the excitation front happen as well, but only after the dynamic electrophysiological inhomogeneity of the medium is well developed, see for example the frame 8540 ms in fig. 3.

The intermediate situation happens if the block of propagation in a particular direction causes a slow down of the front propagation velocity that is not below the critical value. This leads to developing of the local concavities of the front, see fig. 3, and as the propagation conditions improve, the excitation front restores its normal smooth form.

The detailed mechanism of the excitation front dissipation is illustrated on figs. 4 and 5. There we show the evolution of the voltage profile and the fast Na gating variables along selected lines at two selected episodes of the experiment **B**.

On fig. 4, a segment of the excitation front adjacent to the spiral tip dissipates, which leads to a sudden shortening of the front, or, equivalently, a jump of the spiral tip. The selected line crosses that segment, as well as another, surviving site of the excitation front. Thus the one-dimensional profiles show two excitation fronts, propagating rightwards and leftwards, corresponding to the different points of the same front in two dimensions. In the CRN model, the Na^+ current is $I_{Na} \propto \bar{g}_{Na}\, m^3\, h\, j$ where $0 \leq m, h, j \leq 1$ and h and j are fast and slow inactivation gates. The conditions of the front propagation (Biktashev 2002, Biktashev 2003) are determined by the value of the slow Na inactivation gating variable j at the front site. This value is noticeably lower for the rightward front. This leads to the decrease of the Na current, thus slower propagation of the front, thus further decrease of the Na current due to the front moving further into the area with a not fully recovered j and besides, closing of the fast inactivation gate h, until the speed of the front falls below the critical and the Na current is completely blocked. This happens at about 1240ms. After that, the evolution of the transmembrane current at the rightmost segment of the former front is due to passive voltage diffusion and small currents.

On fig. 5, the dissipated segment is in the middle of the front, and this leads to the break of the front onto two pieces with their free ends. Both free ends start acting as a re-entrant source, i.e. the excitation waves start curling around them to form a spiral. Here the newly born spiral waves have soon annihilated and so there was not a multiplication of spiral waves. In both episodes, figs. 4 and 5, the elementary mechanism was dissipation of the front, although the macroscopic effects were different: jump of the spiral tip or birth of a pair of new tips.

Hypermeander of the tip of the spiral. The experiment here lasted long enough to attempt to classify the trajectory of the tip in terms of the theory of meander patterns (Zykov 1986, Barkley, Kness & Tuckerman 1990, Winfree 1991, Biktashev, Holden & Nikolaev 1996, Biktashev & Holden 1998*a*). Being highly irregular and spatially extended, the trajectory observed here should be classified as "hypermeander", as opposed to stationary rotation or biperiodic "regular"

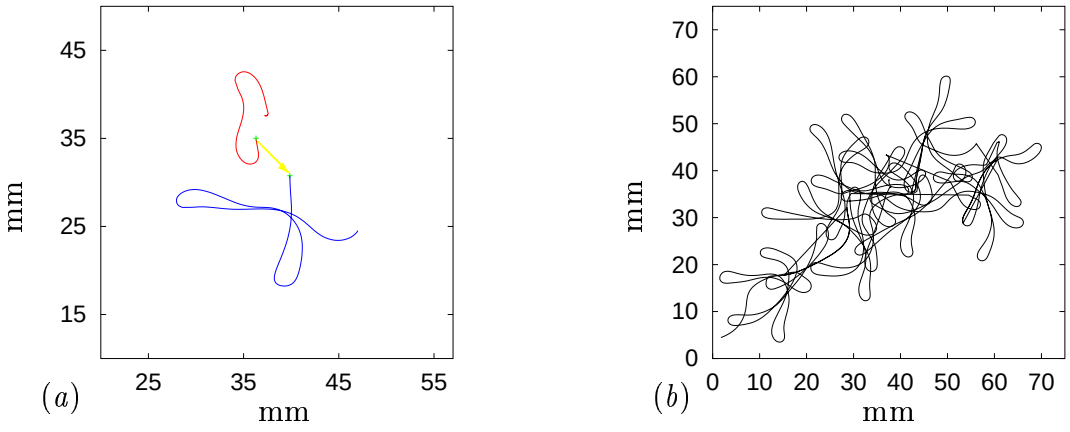

Figure 6: Trajectories of the tips of the spiral waves in the two numerical experiments. (*a*) Trajectory of the tip of the spiral during the first 620 ms of the experiment **A**, with the initial spiral built from long excitation wave obtained by short-time slow pace stimulation. The red line: trajectory of the spiral wave tip for the first 224 ms, until the first dissipation of the excitation front in the vicinity of the spiral core. The yellow arrow indicates *the instantaneous displacement of the tip* due to the front dissipation. The blue line: trajectory of the newly created tip for the next 400 ms, until the beginning of the second dissipation of the excitation front at 624 ms. (*b*) Hypermeander trajectory of the tip of the spiral wave in the experiment **B**, with the initial conditions built from short excitation wave obtained by long-time rapid pace stimulation. The linear intervals in the trajectory correspond to the instantaneous displacements of the tip due to the events of front dissipation.

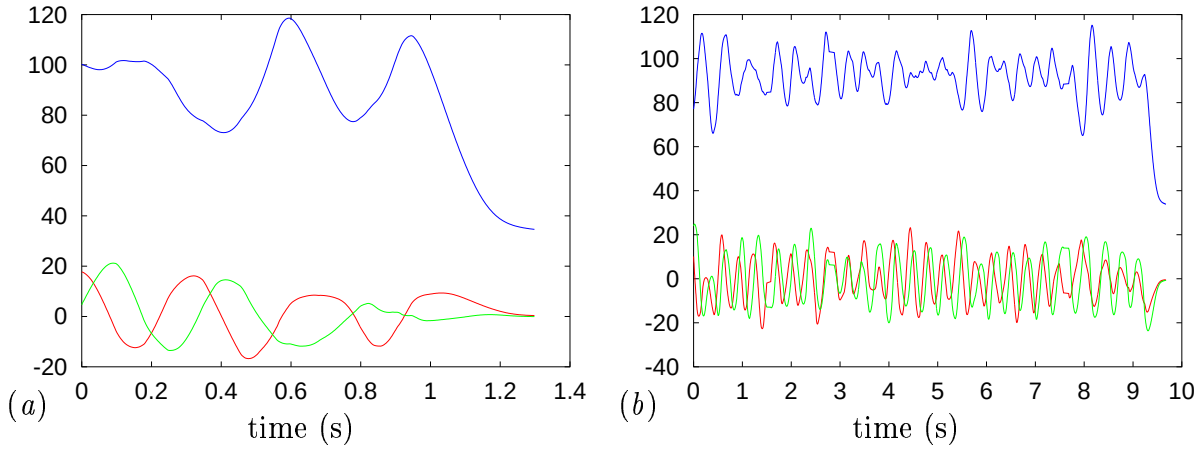

Figure 7: Pseudo-ECGs of the two numerical experiments. Vertical scale is in arbitrary units. The red, green and blue lines correspond to the three 'channels' as described in the text. (*a*) Experiment **A**. (*b*) Experiment **B**. The experiment **A** is too short to classify the ECG. The experiment **B** shows the morphology of a polymorphic tachycardia or fibrillation.

meander.

It was suggested (Clayton, Bailey, Biktashev & Holden 2001) that the spatial extent of meander might play a role in the self-termination of re-entrant arrhythmias. This viewpoint is consistent with the results of this experiment, as here we indeed have a spatially extended tip trajectory that eventually reached the vicinity of the border and annihilated on it. However, getting near to the border is not sufficient for the termination of the spiral. During the experiment the spiral survived after its tip had been closer to the boundary than the last observed point of the trajectory before the complete annihilation. The difference was that these close encounters happened in different evolution phases of the spiral: in the phase of the tip germination, when the tip of the wave made sharp turns, the spiral survived, while the annihilation occurred when that encounter happened during the front dissipation phase, characterised by straight shape of the tip trajectory. So, spiral wave annihilation occurs due to the dissipation of the last piece of the front, the geometric constraints of the proximity to the inexcitable border, or even its corner as in this case, is a facilitating factor.

The pseudo-ECGs of the experiment (fig. 7(b)) resembles the morphology of a polymorphic tachycardia or fibrillation, despite the fact that there is only one spiral wave (apart from short transient after the events of front dissipation). As the ECG is an integral characteristic of a spatially distributed process, its form is a consequence of the complex evolution of the spiral wave including the variety of phenomena described above.

Other experiments. We have also performed five experiments with initial conditions as in Experiment B, with added small perturbations. In four experiments, the perturbation was of the E field (transmembrane voltage) in the form $a\sin(k_1\pi(x-x_{\min})/(x_{\max}-x_{\min}))$ or $a\sin(k_1\pi(x-x_{\min})/(x_{\max}-x_{\min}))\sin(k_2\pi(y-y_{\min})/(y_{\max}-y_{\min}))$ with randomly chosen $a \le 20\,\mathrm{mV}$, $k_{1,2} \le 30$. In one experiment, the perturbation was of the o_i field in the form $0.1\sin(30\pi(x-x_{\min})/(x_{\max}-x_{\min}))\sin(20\pi(y-y_{\min})/(y_{\max}-y_{\min}))$, with o_i clamped afterwards to the $[0,1]$ interval. In all cases, the evolution of the voltage field during the first rotation was visually indistinguishable from Experiment B. Later, however, the evolution diverged completely, although the qualitative features were the same as in Experiment B. In all cases, the re-entry self-terminated, and the lifetime of the re-entry was between 4.452 and 7.878 seconds (6.48 ± 1.38), i.e. shorter than in the experiment B without perturbation. This is consisten with the interpretation of the self-termination as a result of developing functional inhomogeneity, since adding initial inhomogeneity makes it happen sooner.

4 Conclusion.

In the Courtemanche et al. (1998) model, the excitation front breaks due to its local dissipation, where and when it is not able to propagate quickly enough. So the waves break from their heads (excitation fronts), not from their refractory tails, and a piece of tail behind a broken front slowly decay. A commonly adopted operational definition of the break of an excitation wave is reduction to zero of its length, defined as the width of the region with high membrane potential (Weiss et al. 2000). We now argue that this reduction is not the cause of the wavebreak, but a very distant consequence, as at that stage there is no propagating wave as such, i.e. no excitation front, but only a decaying refractory tail. The decaying tails contribute to the electrophysiological inhomogeneity of the medium. Many shadows of such "decaying tails" can be seen in figs. 1, 2, and 3. These can also be observed in many published simulations of fibrillation in biophysically detailed models, see e.g. in the Figure 2.D of (Weiss et al. 2000).

The CRN model, as far as we know, is the first biophysically realistic model that demonstrates hypermeander of spiral wave tip. This spatially extended wandering of the wave tip facilitates the self-termination of re-entry.

The pseudo-ECG of the experiment B shows fibrillation type morphology. This was not a consequence of multiple wavelets, but the dynamic electrophysiological inhomogeneity, including

erratic movement of the re-entry site throughout the tissue (the hypermeander) and irregular occurring triggered recovery.

The model of atrial tissue shows remarkable stability against fibrillation: in all experiments re-entry does not exist indefinitely, but self-terminates within seconds. The exact scenario of the re-entry evolution and its total duration depend on initial conditions. This is consistent with the fact that at standard parameter values, the model is supposed to represent a healthy tissue. The self-termination occurs via development of dynamic electrophysiological inhomogeneity, which leads to the simultaneous dissipation of all excitation fronts of all wavelets existing in the medium.

Acknowledgements. This work was supported in part by grants from EPSRC and MRC (GR/R28935, GR/N04324, GR/S08664/01, G0000315), and by an CVCP ORS award and a Tetley and Lupton Scholarship for IVB.

References

Barkley, D., Kness, M. & Tuckerman, L. S. (1990), 'Spiral-wave dynamics in a simple-model of excitable media - the transition from simple to compound rotation', *Physical Review A* **42**(4), 2489–2492.

Biktashev, V. N. (2002), 'Dissipation of the excitation wavefronts', *Phys. Rev. Lett.* **89**(16), 168102.

Biktashev, V. N. (2003), 'A simplified model of propagation and dissipation of excitation fronts', *Int. J. of Bifurcation and Chaos* . Submitted (in this issue).

Biktashev, V. N. & Holden, A. V. (1996), 'Re-entrant activity and its control in a model of mammalian ventricular tissue', *Proc. Roy. Soc. Lond. ser. B* **263**, 1373–1382.

Biktashev, V. N. & Holden, A. V. (1998*a*), 'Deterministic Brownian motion in the hypermeander of spiral waves', *Physica D* **116**(3–4), 342–354.

Biktashev, V. N. & Holden, A. V. (1998*b*), 'Re-entrant waves and their elimination in a model of mammalian ventricular tissue', *Chaos* **8**, 48–56.

Biktashev, V. N., Holden, A. V. & Nikolaev, E. V. (1996), 'Spiral wave meander and symmetry of the plane', *IJBC* **6(12A)**, 1373–1382.

Clayton, R. H., Bailey, A., Biktashev, V. N. & Holden, A. V. (2001), 'Re-entrant cardiac arrhythmias in computational models of long QT myocardium', *JTB* **208**, 215–225.

Clayton, R. H., Murray, A., Higham, P. D. & Campbell, R. W. F. (1993), 'Self-terminating ventricular tachyarrhythmias – a diagnostic dilemma', *The Lancet* **341**, 93–95.

Cobbe, S. M. (1997), 'Using the right drug - a treatment algorithm for atrial fibrillation', *European Heart Journal* **18, Suppl. C**, C33–C39.

Courtemanche, M., Ramirez, R. J. & Nattel, S. (1998), 'Ionic mechanisms underlying human atrial action potential properties: insights from a mathematical model', *Am. J. Physiol.* **275**, H301–H321.

Gulrajani, R. M. (1998), *Bioelectricity and Biomagnetism*, John Wiley and Sons, New York.

Jalife, J., Berenfeld, O. & Mansour, M. (2002), 'Mother rotors and fibrillatory conduction: a mechanism of atrial fibrillation', *Cardiovascular Research* **54**(2), 204–215.

Leon, L. J., Roberge, F. A. & Vinet, A. (1994), 'Simulation of two-dimensional anisotropic cardiac reentry: effects of the wavelength on the reentry characteristics', *Ann. Biomed. Eng.* **22**, 592–609.

Makikallio, T. H., Huikuri, H. V., Myerburg, R. J., Seppanen, T., Kloosterman, M., Interian, A., Castellanos, A. & Mitrani, R. D. (2002), 'Differences in activation patterns between sustained and self-terminating episodes of human ventricular fibrillation', *Annals of Medicine* **34(2)**, 130–135.

Nygren, A., Leon, L. J. & Giles, W. R. (2001), 'Simulations of the human atrial action potential', *PTRSA* **359**, 1111–1125.

Panfilov, A. & Pertsov, A. (2001), 'Ventricular fibrillation: evolution of the multuple-wavelet hypothesis', *Phil. Trans. Roy. Soc. Lond. ser. A* **359**, 1315–1325.

Weiss, J. N., Chen, P. S., Qu, Z., Karagueuzian, H. S. & A., G. (2000), 'Ventricular fibrillation: How do we stop the waves from braking?', *Circ. Res.* **87**, 1103–1107.

Winfree, A. T. (1991), 'Varieties of spiral wave behavior in excitable media', *Chaos* **1**(3), 303–334.

Zykov, V. S. (1986), 'The cycloid circulation of spiral waves in the excitable medium', *Biofizika* **31**(5), 862–865. in Russian.